Available online at www.sciencedirect.com

ScienceDirect

Scripta Materialia 82 (2014) 21–24

Scripta MATERIALIA

www.elsevier.com/locate/scriptamat

Early-stage detection of surface stress corrosion cracking at the subgranular level

Aurélie Clair,[a,b] Marc Foucault,[b] Olivier Calonne[b] and Eric Finot[a,*]

[a] *Laboratoire Interdisciplinaire Carnot de Bourgogne, UMR 6303 CNRS, Université de Bourgogne, F-21078 Dijon, France*
[b] *Areva ANP, Centre Technique Département Corrosion-Chimie, BP 181, 71205 Le Creusot, France*

Received 24 December 2013; revised 7 March 2014; accepted 10 March 2014
Available online 24 March 2014

The strain field at the interface between an alloy and its oxide layer has been mapped using nanopatterned gauges resistant to the environment of the primary nuclear medium. It was found that oxidation has decreased the alloy ductility, thereby enabling some grain boundary opening to be detectable from 1.8% strain. It is shown that statistics of extreme rare events of hotspots quantify the occurrence of the local opening of intergranular cracks, and thereby the ageing process.

Keywords: Corrosion; Nickel alloy; Statistics; Nanoscale surface deformation; Cracking

The brittleness of a material caused by the mechanical action induced by oxidation is not properly understood. Given the substantial hazard to safety and economic performance, in addressing the challenges facing the nuclear industry, controlling the ageing process and the failure of materials is very important for the durability of structural components [1]. Despite the complexity of the underlying mechanisms and the experimental difficulties encountered in pressurized water reactors (PWR), evaluations of the safety criteria and lifetime of a nuclear power plant are crucial [2,3]. The cracking of alloy 600 components, such as steam generator tubes and welds, was correlated to the formation of a chromium-rich oxide film [4–6] on the inner surface of the alloy.

Understanding the role of the oxide layer is thus essential to provide criteria for the assessment of crack initiation [7,8]. Numerous studies have been conducted on the crack initiation [9–11], but there are few publications reporting experiments on the mechanical impact induced by the oxide layer [12]. The mechanical parameters of α-Cr_2O_3 films were measured by Raman spectroscopy [13]. Large grain-to-grain variations in the compressive residual strains of oxidized metals were first revealed by X-ray diffraction [14]. Failure induced by intergranular cracking in the presence of hydrogen [15] was observed and a neutron diffraction method has also shown the intergranular strains [16]. More recently, the stress corrosion cracking of alloy 600 observed by transmission electron microscopy was correlated with the strain concentration at grain boundaries before the oxidation, as imaged by electron backscattering diffraction (EBSD) [17]. Unfortunately, given the changes in surface roughness, EBSD is not suitable to monitor changes in the strain field for large-scale kinetics.

Crack inspection is currently at the millimetre scale [18]. The appearance and propagation of cracks (crack length and growth rate) are usually analysed using statistical spatial distribution [19]. The statistical model for fracture toughness has been described either by a Weibull probability function [20] for the fracture properties or as an alternative by the Burr function [21]. The prediction requires clarification at an early stage of the occurrence of apertures in grain boundaries and the contributing factors. Hence, we face a more fundamental problem for quantifying the conditions under which the cracking occurs at the subgranular scale. Concepts of rare events and extreme values [22] are set out in engineering for failure of complex technological devices. However, this notion was not applied to the cracking interfaces at the granular level.

The overall aim of the present work is to find an experimental way to quantitatively assess the influence of the oxidation process on mechanical material

---

[*] Corresponding author. Tel.: +33 3 80 39 3774; fax: +33 3 80 39 60 24; e-mail: eric.finot@u-bourgogne.fr

http://dx.doi.org/10.1016/j.scriptamat.2014.03.010
1359-6462/

weakening. We have used nanopatterning techniques to fabricate nanoscale gauges that have proved to be useful for obtaining information at the subgranular mechanical scale [23,24]. A substantial number of gauges give us access to rare events. These gauges were found to withstand the aggressive oxidizing environment of the primary medium of a power plant. The mechanical effect of gradual traction on local plastic deformations was then monitored until intergranular cracks opened up. Our study shows that the statistical distribution of the maximum shear strain ε_{max} [23] brings new prospects for analysing the local opening up of grain boundaries. We propose the Burr statistics, not only to represent both the chemical and mechanical effects, but also to estimate rare events corresponding to the hotspots of the highest deformations.

The tensile specimens of alloy 600 were obtained from components of nuclear power plants [25]. Samples were first machined into a 30 mm long dog-bone shape. The initial stage was to select some grain boundaries over an area of interest presenting various activities towards both the corrosion process and the further tensile test. EBSD was first used to evaluate the microstructure of the surface and, more specifically, to determine the crystallographic orientation of the grain boundaries (GBs). The GBs are indicated on the EBSD map (Fig. 1) by white arrows. GB1 and GB3 are grain boundaries $\Sigma3$ with angular misorientations θ of 59.6° and 55.6°, respectively. GB4 is classed as type $\Sigma3\Sigma45$, with $\theta = 36.8$. GB2, GB5, GB6 and GB7 fall into an undetermined category, with $\theta = 37.6°, 51.2°, 54.7°, 28.8°, 37.6°$. The coincident site lattice of type $\Sigma3$, such as GB1 and GB3, is deemed to resist stress corrosion cracking, contrary to the undetermined GBs [17].

Arrays of $[1000 \times 1000]$ nanodots were then deposited in the area of interest by e-beam lithography, as described previously [23]. The gauge lengths $L_x = L_y = 1\mu m$ were chosen to set a minimum of 100 dots per grain. Particular attention was paid to the issue of nanodot stability in the corrosive environment. Gold nanodots of 140 nm diameter were deposited using 5 nm chromium as an anchoring layer. The nanodot height was adapted to be at least 3 × the thickness of the corrosion layer, which was estimated to be 15 nm by spectroscopic ellipsometry [26].

The sample was then oxidized in a static titanium autoclave containing simulated PWR primary water at 325 °C and 155 bar, as described by Panter et al. [4]. Nanogauges without any external tensile stress enable accurate measurements of the surface distribution of the corrosion-induced strain (Fig. 2a). The surface strain tensor $(\varepsilon_{xx}, \varepsilon_{yy}, \gamma_{xy})$ was deduced from the difference between the gauge lengths $(L_{xi}, L_{yi}, L_{xf}$ and $L_{yf})$ orientated along the x and $y$directions and the cell angles (θ_i and θ_f) measured before (index i) and after (index f) the tensile loading. The maximum principal shear strain ε_{max} was deduced from $\varepsilon_{xx} = ln\left(\frac{L_{xf}}{L_{xi}}\right), \varepsilon_{yy} = ln\left(\frac{L_{yf}}{L_{yi}}\right), \gamma_{xy} = tan(\theta_i - \theta_f)$ using:

$$\varepsilon_{max} = \frac{1}{2}\sqrt{(\varepsilon_{xx} - \varepsilon_{yy})^2 + \gamma_{xy}^2} \qquad (1)$$

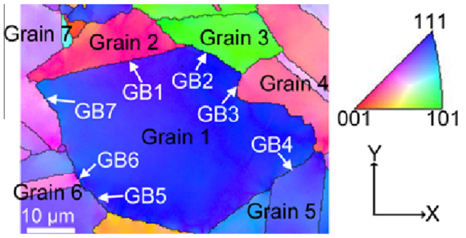

Figure 1. EBSD image defining the grains and the GBs.

No indications of a relationship between the highest surface deformation and the microstructure were reported in the EBSD results. The oxidation induces a relative spatially homogeneous shear strain, estimated to be 2.2%. The corrosion-induced strain may arise from two main sources: the thermal strain and the difference between the thermal expansion coefficients of the sample and the oxide layers. The growth distortion (epitaxy, volume change) results from the lattice mismatch at or near the interface between the oxide and the alloy. In our particular case, the mixed growth, namely both anionic and cationic processes, locks the oxide layer in a compressive state and therefore the alloy substrate in a tensile state. A loss of chromium in the underlying alloy substrate [4] decreases the lattice parameters of the alloy, thereby leading to a compressive stress.

The induced weakening of the mechanical properties of the surface was then investigated by locally inspecting the opening of a preoxidized grain boundary as a function of the progressive applied tensile loading. Without preoxidation in the autoclave, our last results [23] show that the highest strain was mainly concentrated at the GBs; however, no opening of grain boundary was observed (the cracking of unoxidized alloy 600 occurs when loading with applied tensile strain exceeds 15%). Figure 2 shows the spatial distribution of the shear strains during the tensile test of the oxidized sample. The highest values are not concentrated exclusively at the grain boundaries; some intragranular shear bands are observable at the lowest tensile excitation. The oxidation makes the *GBs* fragile, facilitating their opening, as observed by high-resolution scanning electron microscopy (SEM) (Fig. 4). Boundary openings can then be collocated by SEM and strain imaging, and are marked by solid black curves in Figure 2b. The opening dots named O_1, O_3 and O_6 appeared first along GB3, GB4 and GB7, respectively, and were initiated at 1.8%. Other openings (O_2, O_4 and O_5) were only visible above 7%. Those cracks are highly disoriented towards the tensile axis. Given the grain rotations, the tensile axis differs from

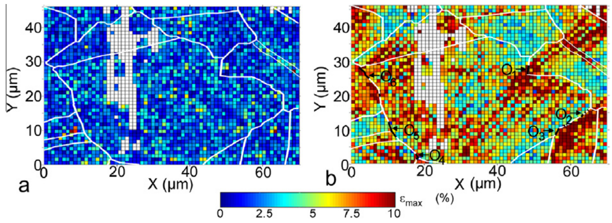

Figure 2. Map of the shear strain ϵ_{max} of the alloy 600 oxidized for 250 h in a PWR (325 °C, 155 bar, $p(H_2) = 0.3$ bar) (a) and then loading with applied tensile strain of 7.1% (b). Pixels that could not be analysed were left blank.